# Driving forces and charge-carrier separation in p-n junction solar cells

Cite as: AIP Advances 9, 055026 (2019); doi: 10.1063/1.5092948
Submitted: 15 February 2019 • Accepted: 15 May 2019 •
Published Online: 28 May 2019



Benjamin Lipovšek,[a] Franc Smole, Marko Topič, Iztok Humar, and Anton Rafael Sinigoj

## AFFILIATIONS

University of Ljubljana, Faculty of Electrical Engineering, Tržaška 25, 1000 Ljubljana, Slovenia

[a]Corresponding e-mail: benjamin.lipovsek@fe.uni-lj.si

## ABSTRACT

While p-n junction solar cells have long been established as the dominant solar-cell technology in the market, the origin of the charge-carrier separation in these devices remains open to debate. It is often attributed to the built-in electric field that exists across the junction in thermodynamic equilibrium, although this interpretation can lead to physical inconsistencies. In this work we present an interpretation approach based on the analogy between a solar cell and a generalized electric source model. Our interpretation is given through a detailed analysis of the electric potential and the non-electric chemical potential across each device, which are plotted together in complete potential diagrams introduced for this purpose. We demonstrate that the driving force separating the free charge carriers in both devices originates from the change of the non-electric chemical voltage that happens once the device is brought out of thermodynamic equilibrium. This change, therefore, can be interpreted as the driving force that triggers the selective motion of charge carriers and, thus, induces the electric voltage at the terminals of the device.



## I. INTRODUCTION

The field of photovoltaics is seen as one of the key players in meeting the ever-increasing global demands for sustainable electric energy. While many different solar-cell technologies have emerged over the years, modern technologies based on crystalline silicon p-n junction solar cells (BSF, PERC, PERT, PERL, EWT, IBC) still account for almost 95% of the total production.[1] However, while the basic theory of p-n junction solar cells was established decades ago, the interpretation of certain aspects of these devices remains open to debate.[2]

One such open question is the origin of the photo-generated charge-carrier separation that takes place in an illuminated p-n junction solar cell. The explanation most widely put forward in the majority of textbooks and lecture halls is the one that connects this phenomenon to the built-in electric field $\mathbf{E}_{bi}$ that pre-exists across the p-n junction in thermodynamic equilibrium (in the dark). Specifically, as the excess charge carriers (free electrons and holes) are generated under illumination, this electric field is thought to drive the free electrons into the n-type region and the holes into the p-type region, as shown schematically in Fig. 1. Thus, a constant voltage between the terminals is established, and a constant current flows out of the solar cell and over the load.

There are a number of physical inconsistencies in this interpretation. The first is the fact that the built-in field $\mathbf{E}_{bi}$ exists in the state of thermodynamic equilibrium. In this state, all the forces and fields over the p-n junction – including the built-in field – are in complete balance (i.e. the electric forces are in balance with the opposing non-electric forces). In order to break this balance and, thus, initiate the flow of charge carriers, some change of any or all of these forces and fields needs to appear. Therefore, it is this *change* which terminates thermodynamic equilibrium that should be held responsible for driving the charge carriers over the p-n junction, and not the initial forces and fields which are inherently balanced out.

Further inconsistencies arise from the fact that the built-in electric field $\mathbf{E}_{bi}$ (as well as every other electric field in the circuit in Fig. 1) is a *Coulomb field*, which is a *conservative* field for which $\oint \mathbf{E}\cdot d\mathbf{l} = 0$. First, from Fig. 1, it can be seen that the built-in electric field $\mathbf{E}_{bi}$ and the current $I$ flowing across the p-n junction are oriented in the same direction, which is a property common to a load, not a source. Second, the integral of the electric field along the closed loop in Fig. 1 would yield a non-zero result, $\oint \mathbf{E}\cdot d\mathbf{l} \neq 0$, since $\mathbf{E}_{bi}$ and $\mathbf{E}_{R}$,

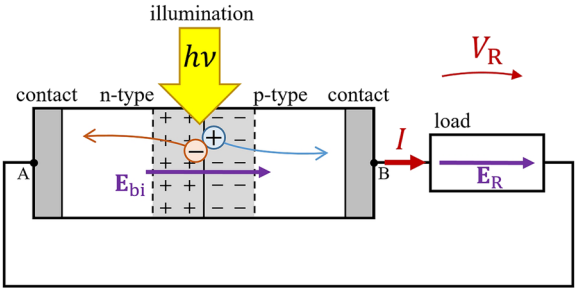


**FIG. 1**. Schematic of the common interpretation of the p-n junction solar-cell operation.

the electric field inside the load, are oriented in the same direction. And third, the work done by a conservative field along a closed loop should always be zero. Therefore, we cannot expect that the built-in field $\mathbf{E}_{bi}$ would be able to sustain a constant current flowing through the circuit in Fig. 1, resulting in a constant dissipation of heat on the load.

A physically more consistent interpretation of this phenomenon has been proposed most prominently by Würfel *et al.*,[3,4] and also by Green *et al.*[5] and others.[6–8] They demonstrated that the mechanism of charge-carrier separation should instead be attributed to the *non-electric forces* existing across the p-n junction which are related to the concentrations of charge carriers. However, despite the fact that this alternative explanation complies with the laws of physics and avoids the contradictions discussed above, the majority of the broader photovoltaics community still favours the interpretation based on the built-in electric field.

Therefore, in this work we add to the previous publications our own explanatory approach by which we aim to further clarify the origins of the driving forces acting on the photo-generated charge carriers in an illuminated p-n junction solar cell. Our goal is to provide, in one place, a physically consistent and self-contained interpretation of selective charge-carrier separation. We build the case ground-up from fundamentals, which is why even some of the more basic principles of semiconductor materials are included for the sake of completeness.

In our interpretation we draw on the close analogy between a solar cell and an arbitrary generalized electric source, which is discussed first. We focus on the relation between the existing electric and non-electric forces in the device and how they influence the motion of charge carriers. Next, to visualize this motion, we detract from the conventional energy diagrams and instead introduce the *complete potential diagrams* that provide the full picture of the potential distribution in the solar cell, either in the dark or under illumination. Using these diagrams as well as the derived theoretical formulations, we finally demonstrate that the driving force acting on the charge carriers is clearly *non-electric* in nature and inherently *selective*. It originates from the change of the chemical potential difference across the p-n junction that happens once the solar cell is illuminated and brought out of thermodynamic equilibrium.

## II. GENERALIZED ELECTRIC SOURCE MODEL

The motion of charge carriers inside a closed system is driven by the tendency to reduce the *free potential energy* of the system, often called the Gibbs energy, $G$.[9] The Gibbs energy of charge carriers can, in general, be composed of many terms related to various variable physical quantities. At constant temperature and constant volume, however, it can be narrowed down to the combination of the chemical and the electric potential energies.[3] With respect to the reference zero energy of a completely free carrier at rest, the Gibbs energy of negative charge carriers in materials (e.g. electrons in semiconductors) is negative, while the Gibbs energy of positive charge carriers in materials (e.g. holes in semiconductors) is positive.

Associated with the Gibbs energy, we can define the net *potential* of the charge carriers $\phi_{net}$, as given in Eq. 1, where $\pm q$ is the elementary charge. We can further define the net *driving force* $\mathbf{F}_{net}$ that acts on the charge carriers in the direction of a decreasing free potential energy (negative gradient), as given in Eq. 2, and the net *driving field* $\mathbf{E}_{net}$, as given in Eq. 3. Since both $\mathbf{F}_{net}$ and $\mathbf{E}_{net}$ can be highly nonhomogeneous in realistic systems, it is also convenient to define the net *potential difference* $V_{net}$ between any two selected points in the system. In our work, $V_{net}$ and any other potential differences will be referred to as *voltages*. They will be calculated by the line integration of $\mathbf{E}_{net}$ between the two selected points, as given in Eq. 4.

$$\phi_{net} = \frac{1}{\pm q} G \tag{1}$$

$$\mathbf{F}_{net} = -\nabla G \tag{2}$$

$$\mathbf{E}_{net} = \frac{1}{\pm q} \mathbf{F}_{net} = -\nabla \phi_{net} \tag{3}$$

$$V_{net} = \int_P^Q \mathbf{E}_{net} \cdot \mathbf{dl} = \phi_{net,P} - \phi_{net,Q} \tag{4}$$

The most important quantity that we will focus on in the scope of this work is the net *potential* (in volts). First, it can be observed from Eq. 1 that the potential of negative and positive charge carriers in materials is always positive (with respect to the reference zero potential of a completely free carrier at rest). Second, from the above equations it is evident that the net field and the net voltage (the two quantities most closely related to the electric current) depend directly on the net potential: $\mathbf{E}_{net}$ is related to the negative *potential gradient* at a certain point in the system, and $V_{net}$ to the *potential difference* between two points in the system (Eqs. 3 and 4). Further on, if we decompose the net potential into the *non-electric* potential $\psi$ and the *electric* potential $\phi$, so that $\phi_{net} = \psi + \phi$, the nature of these fields and voltages is also revealed. And finally, we will demonstrate that plotting the spatial distributions of these potentials can be a powerful visualization tool for understanding the motion of charge carriers in such systems. In the scope of our work these plots will be introduced and referred to as the *complete potential diagrams*.

First, consider an arbitrary homogeneous open system in which there is no generator action taking place. The system is in complete equilibrium with no forces whatsoever acting on the charge carriers. The complete potential diagram for this system is presented in Fig. 2; the potentials $\psi^0$ and $\phi^0$ are represented by full black lines (the superscript "0" indicates the situation with no generator action). It is clear that neither potential is changing with the

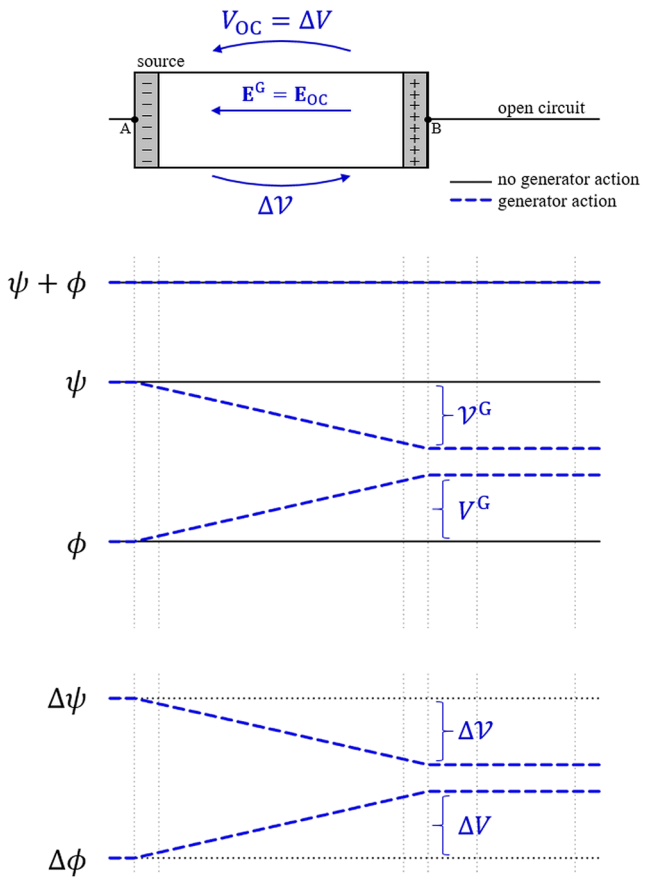


**FIG. 2**. Complete potential diagram of a linear electric source in the state of no generator action (full black lines), and under open-circuit conditions (dashed blue lines). The diagram is shown for the source only (open system).

position inside the system; the absence of any potential gradients indicates that there are no forces or fields of any kind acting on the charge carriers at any point in the system, while a zero potential difference between the two terminals (points A and B in Fig. 2) indicates that there is no resultant voltage maintained across the system.

Next, suppose that some form of generator action (mechanical, chemical, thermal, etc.) is suddenly enabled which terminates the equilibrium of the system. Suppose also that in this short amount of time the charge carriers have not yet been able to separate, which means that the electric potential remains constant throughout the system. The driving force (often referred to as the *electromotive* force[10]) acting on the charge carriers at this point therefore must be *non-electric* in nature; it originates from the gradient of the *non-electric* potential $\psi^G$ which is now no longer constant (the superscript "G" indicates the generator action conditions). In our generalized case we consider a simple linear electric source with a linear spatial distribution of $\psi^G$, as shown in Fig. 2. It is important to note, however, that this choice is completely arbitrary and has no influence on the physical principles that we aim to emphasize in this work.

The motion of charge carriers is now initiated under the influence of the *non-electric* driving field $\boldsymbol{\mathcal{E}}^G$. Since the field is oriented along $-\nabla\psi^G$ according to Eq. 3, the positive charge carriers in Fig. 2 would be driven to the right, and the negative to the left. This *selective* motion of charge carriers breaks electric neutrality. The electric potential $\phi^G$ is no longer constant; an additional *electric* field $\mathbf{E}^G$ is generated in an opposite direction that works to suppress further charge-carrier separation. If the source is not connected to a load, a new balance is eventually established in which there is zero net field acting on the charges. This situation is commonly known as the *open-circuit* (OC) conditions.

The complete potential diagram for this case is plotted in Fig. 2. The potentials $\psi^G$ and $\phi^G$ are represented by dashed blue lines. The gradient of $\psi^G$ is matched by the opposite gradient of $\phi^G$, which means that there is zero net field acting on the charges; $\mathbf{E}^G_{net} = \boldsymbol{\mathcal{E}}^G + \mathbf{E}^G = \mathbf{0}$. Also matched are the potential differences between the terminals, which illustrates the balance of voltages; $V^G_{net} = \mathcal{V}^G - V^G = 0$. The electric voltage measurable at the terminals of the source can be written as $V^G = V_{OC} = \mathcal{V}^G$, where $V_{OC}$ stands for the open-circuit voltage. And finally, since the net potential $\phi^G_{net} = \psi^G + \phi^G$ is constant throughout the device, its zero gradient again indicates that there is zero net driving field acting on the charge carriers and, consequently, there is no resultant electric current flowing through the system.

From the above discussion it might appear that the motion of the charge carriers and the open-circuit voltage $V_{OC}$ are triggered directly by the total non-electric voltage $\mathcal{V}^G$ that exists between the two terminals. For the sake of generality, however, it is crucial to emphasize that these processes are induced rather by the *change* that happened to the system when the generator action was enabled and the system was brought out of equilibrium. For this reason it is beneficial to plot also the changes of the potentials in the complete potential diagrams, i.e., $\Delta\psi = \psi^G - \psi^0$ and $\Delta\phi = \phi^G - \phi^0$, as shown in the bottom part of Fig. 2. For the particular case of the linear electric source discussed here, the changes of the fields and voltages indeed match the total voltages between the terminals, $\Delta\mathcal{V} = \mathcal{V}^G - 0 = \mathcal{V}^G$ and $\Delta V = V^G - 0 = V^G$, so plotting them may seem redundant. However, this is not necessarily the case in other types of electric sources, which will be evident especially for the illuminated p-n junction solar cell, so we plot $\Delta\psi$ and $\Delta\phi$ in all the potential diagrams for the sake of consistency. In general, it is therefore more appropriate to express the open-circuit voltage as $V_{OC} = \Delta V = \Delta\mathcal{V}$. The separation of the charge carriers that led to the formation of the electric voltage $V_{OC}$ at the terminals of the electric source was triggered solely by the *change* of the *non-electric* voltage $\Delta\mathcal{V}$, whereas the *initial* (equilibrium) values of the non-electric and electric voltages are of no relevance whatsoever.

If we connect the source to a load, such as the linear resistor shown in Fig. 3, the charges can flow out of the source through the load. This flow reduces the build-up of electric charges at the terminals of the source and, consequently, changes the electric field, $\mathbf{E}^G = \mathbf{E}_{OC} + \delta\mathbf{E}$. Since the field is reduced, the change $\delta\mathbf{E}$ is oriented in the opposite direction than $\mathbf{E}_{OC}$. The voltage at the terminals is reduced as well, $V^G = V_{OC} - \delta V$, where $\delta V$ is calculated by the line integration of $\delta\mathbf{E}$ along its direction. The net field acting on the charge carriers inside the source becomes non-zero, $\mathbf{E}^G_{net} = \boldsymbol{\mathcal{E}}^G + \mathbf{E}^G \neq \mathbf{0}$, and so does the net voltage, $V^G_{net} = \mathcal{V}^G - V^G = \mathcal{V}^G - (V_{OC} - \delta V) = \delta V$. This resultant net voltage $\delta V$ which is *inside* the source oriented in the *opposite*

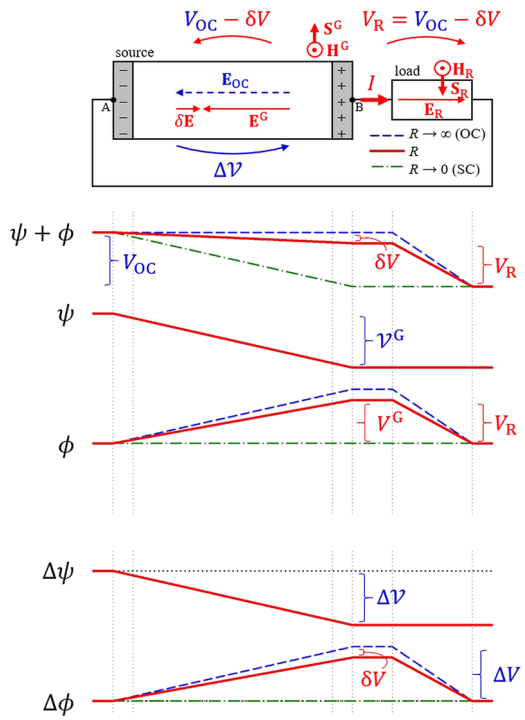


**FIG. 3**. Complete potential diagram of a linear electric source in open-circuit (dashed blue lines), in short-circuit (dash-dotted green lines), and connected to a load (full red lines).

direction of the voltage at the terminals $V^G$ is what drives a constant flow of charges through the electric circuit. The rate of this flow is limited by the rate at which the charges can depart from the terminals, which is governed by the current-voltage characteristics of the load (in our case the resistance $R$; $I = V_R/R$ where $V_R = V^G$), as well as by the rate at which the departed charges can be replenished, which is governed by the *internal* current-voltage characteristics of the source (in our case the internal resistance $R_g$; $I = \delta V/R_g$). Eventually, a new balance is established with a constant current $I$ flowing through both the source and the load.

If the resistance of the load is reduced to zero, $R \to 0$ and $V_R \to 0$, the source is put in *short-circuit* (SC) conditions. In this case, the current is limited only by the properties of the source itself. While the *external* voltage at the terminals $V^G$ drops to zero, the *internal* driving voltage inside the source becomes $\delta V_{SC} = V_{OC} - 0 = V_{OC}$. The magnitude of the open-circuit voltage therefore drives the short-circuit current through the source in short-circuit conditions; $V_{OC}$ and $I_{SC}$ are related directly via the *internal* current-voltage characteristics of the source, $I_{SC} = \delta V_{SC}/R_g = V_{OC}/R_g$.

All of the above is also apparent from the complete potential diagram shown in Fig. 3, which is plotted for the complete system (closed loop). The potentials $\psi^G$ and $\phi^G$ are plotted by full red lines for the case of a loaded source, and by dash-dotted lines for the short-circuit conditions. The reduced gradient of $\phi^G$ indicates a reduced field $\mathbf{E}^G$ and, thus, a reduction of the voltage $V^G$. More importantly, however, we can observe that the net potential is no longer constant, which indicates a preferential motion of charge carriers through the system – a net electric current. The current through the source is governed by $\delta V$ (and $\delta\mathbf{E}$) *inside* the source, and that through the load by $V_R$ (and $\mathbf{E}_R$). In open-circuit conditions, $\delta V$ is zero while $V_R$ is equal to $V_{OC}$. In short-circuit conditions, $\delta V$ reaches $V_{OC}$ while $V_R$ drops to zero. In all cases, voltages (and fields) can be deduced by observing the net potential differences (and the net potential gradients) in the respective regions.

Finally, note that the direction of the current flowing through the load is the same as the direction of the electric field $\mathbf{E}_R$ (and voltage $V_R$) over the load. If we also envision the direction of the encircling magnetic field $\mathbf{H}_R$ and the Poynting vector $\mathbf{S}_R = \mathbf{E}_R \times \mathbf{H}_R$ (also drawn in Fig. 3), we see that the electric energy is "flowing in" – it is being *dissipated* in the load. On the other hand, the direction of the current flowing through the source is *opposite* to the direction of the electric field $\mathbf{E}^G$ inside the source; the Poynting vector $\mathbf{S}^G = \mathbf{E}^G \times \mathbf{H}^G$ is oriented outwards, which means that the electric energy is "flowing out" – it is being *generated* by the source.

## III. ON CONSERVATIVE AND NON-CONSERVATIVE FIELDS

Before moving on from the arbitrary electric source to the p-n junction solar cell, we briefly revisit the properties of conservative and non-conservative fields, especially in relation to the proper interpretation of the complete potential diagrams presented in this work.

Suppose that the resistor in Fig. 3 is replaced by a voltmeter. Suppose also that the voltmeter is ideal (infinite internal resistance), which puts the electric source in open-circuit conditions, and that the probes of the voltmeter as well as the terminals of the source are fabricated from the same metal material (although the main points of the following discussion would apply also if that was not the case). It is generally acknowledged that the voltmeter in this situation measures the *net* potential difference (voltage) between terminals B and A. However, due to the nature of non-conservative fields influencing the system, this difference *depends on the path taken from point B to point A*. This is a highly nonintuitive concept that has been recognized also in other fields of physics,[11] yet it is crucial for proper interpretation of the complete potential diagrams.

Along the path with the electric source (battery, thermocouple, solar cell, etc.), there exists a non-electric voltage between the terminals A and B which is established by non-electric forces inside the source. As a result, there also exists an opposite electric voltage between the terminals B and A so that the net voltage is zero (open circuit conditions), as described previously. Along the path of the voltmeter, on the other hand, there exists an electric voltage between the probes B and A that matches the electric voltage across the source, so that the sum of all electric voltages in the closed loop of the circuit is zero (Kirchhoff's law), or $\oint\mathbf{E}\cdot\mathrm{d}\mathbf{l} = 0$. This is the fundamental property of *conservative* electric fields. The non-electric voltage between the probes (outside the source), however, is *zero*, since the probes are made of the same material and there are no other electric sources present along this path. Therefore, the sum of all non-electric voltages in the closed loop of the circuit is *not* zero, or $\oint\boldsymbol{\mathcal{E}}\cdot\mathrm{d}\mathbf{l} \neq 0$, which is the fundamental property of *non-conservative* non-electric fields for which Kirchhoff's low *does not apply*.

The net field $\mathbf{E}_{net}$, being the sum of the conservative field $\mathbf{E}$ and the non-conservative field $\boldsymbol{\mathcal{E}}$, is by nature also non-conservative.

Therefore, for the net potential, the Kirchhoff's law does not apply either, which means that the net voltage along one path between any two points in the circuit generally *does not match* the net voltage between the same two points along a different path.

The above is clear also from the complete potential diagram plotted in Fig. 3 (and later on also Fig. 6). In the situation presented for the open circuit conditions (dashed blue lines), the net voltage between B and A is *zero* across the electric source, yet *non-zero* across the voltmeter. The voltmeter measures the net voltage *between the probes*, and since there is no non-electric voltage between the probes along the path with the voltmeter, it effectively measures only the electric voltage.[12] And similarly for the case with the resistor (red lines), the net voltage across the source *does not* match the net voltage across the resistor, which is again purely electric in nature due to the same reasons as in the case of the voltmeter. Only *electric* voltages, in compliance with the conservative nature of the electric fields, obey the Kirchhoff's law, so that the electric voltage across the resistor matches the electric voltage across the source, $V_R = -V^G$.

## IV. SOLAR CELL AS AN ELECTRIC SOURCE

The two types of charge carriers relevant in semiconductor materials are the free electrons in the conduction band with the charge $-q$ and concentration $n$, and the free holes (the absence of electrons) in the valence band with the charge $+q$ and concentration $p$. For the most part they can be treated independently. The concentrations $n$ and $p$ define the chemical *potential energies* $\mu_e$ and $\mu_h$ of the respective carriers, indicated by the subscripts "e" and "h", as given in Eq. 5. The $\tilde{\mu}_e$ and $\tilde{\mu}_h$ are the reference energies at temperature $T = 0$ K, $k$ is the Boltzmann constant, and $N_C$ and $N_V$ are the effective densities of states of the conduction and valence bands, respectively.

$$\begin{aligned} \mu_e &= \tilde{\mu}_e + kT \ln \frac{n}{N_C} \\ \mu_h &= \tilde{\mu}_h + kT \ln \frac{p}{N_V} \end{aligned} \tag{5}$$

Besides the energy, it is again convenient to define the chemical *potential* $\psi$ (in volts). This can be done separately for electrons and holes, as given in Eq. 6.

$$\begin{aligned} \psi_e &= \frac{1}{-q}\mu_e = -\frac{\tilde{\mu}_e}{q} - \frac{kT}{q} \ln \frac{n}{N_C} \\ \psi_h &= \frac{1}{q}\mu_h = \frac{\tilde{\mu}_h}{q} + \frac{kT}{q} \ln \frac{p}{N_V} \end{aligned} \tag{6}$$

In an isolated homogeneous semiconductor material in thermodynamic equilibrium, the charge carrier concentrations are constant, which results in constant chemical energies and chemical potentials throughout the volume. The absence of any potential gradients or potential differences indicates that there are no fields or voltages acting on the charge carriers.

### A. p-n junction in the dark

In the proverbial formation of the p-n junction "in the dark" (without illumination), when the p-type and n-type doped semiconductor layers are "brought into contact" at constant temperature, pressure, etc., the chemical potential $\psi^0$ is no longer constant; for both the electrons and holes it is much higher on the p-type side and lower on the n-type side (the superscript "0" indicates the situation in the dark). This steep gradient of $\psi^0$ induces a *non-electric* (chemical) driving field $\boldsymbol{\mathcal{E}}^0$ that strives to minimize the chemical potential energy of the system. A *non-electric* (chemical) voltage $\mathcal{V}^0_{pn}$ appears across the p-n junction, which can be expressed from the difference of the chemical potential between one and the other side of the junction. In Eq. 7, this is given separately for the electrons and holes. The subscripts "p" and "n" indicate the p-type and the n-type layer, respectively.

$$\begin{aligned} \mathcal{V}^0_{pn,e} &= \psi^0_{p,e} - \psi^0_{n,e} = -\frac{kT}{q} \ln \frac{n^0_p}{N_C} + \frac{kT}{q} \ln \frac{n^0_n}{N_C} = \frac{kT}{q} \ln \frac{n^0_n}{n^0_p} \\ \mathcal{V}^0_{pn,h} &= \psi^0_{p,h} - \psi^0_{n,h} = \frac{kT}{q} \ln \frac{p^0_p}{N_V} - \frac{kT}{q} \ln \frac{p^0_n}{N_V} = \frac{kT}{q} \ln \frac{p^0_p}{p^0_n} \end{aligned} \tag{7}$$

Influenced by these *non-electric* chemical fields and voltages, the charge carriers tend to migrate from regions of high to regions of low concentration; the electrons are being driven from the n-type into the p-type layer, and holes from the p-type into the n-type layer. This motion is called *diffusion*.

As a consequence of the charge-carrier diffusion, the electric neutrality in the vicinity of the p-n junction (the "space-charge" region) is disturbed. The electric potential $\phi^0$ is no longer constant, which induces an electric field $\mathbf{E}^0$ that works to oppose further charge-carrier migration. Eventually, both fields are balanced out, $\mathbf{E}^0_{net} = \boldsymbol{\mathcal{E}}^0 + \mathbf{E}^0 = \mathbf{0}$, and there is no resultant current flowing in either direction. In other words, the charge carriers can no longer reduce their potential energy by migration, since reducing the chemical potential energy now requires an increase of the electric potential energy for the same amount. The "built-in" electric voltages across the p-n junction $V^0_{pn,e}$ and $V^0_{pn,h}$ that compensate the chemical voltages $\mathcal{V}^0_{pn,e}$ and $\mathcal{V}^0_{pn,h}$, respectively, can be expressed directly from $V^0_{net,pn,e} = \mathcal{V}^0_{pn,e} - V^0_{pn,e} = 0$ and $V^0_{net,pn,h} = \mathcal{V}^0_{pn,h} - V^0_{pn,h} = 0$, which leads to $V^0_{pn,e} = \mathcal{V}^0_{pn,e}$ and $V^0_{pn,h} = \mathcal{V}^0_{pn,h}$.

For the case of an example simplified solar-cell structure, this balance is shown schematically by the potential diagram plotted in Fig. 4. All the gradients and differences in the chemical potential

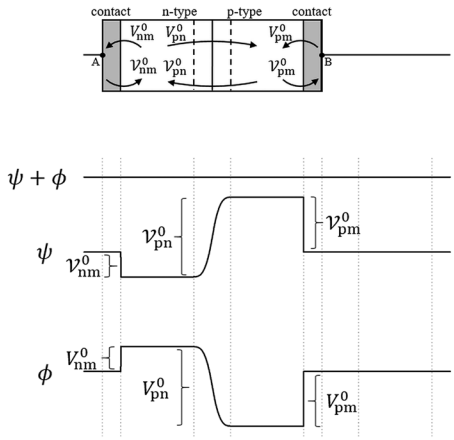


**FIG. 4.** Potential diagram of the p-n junction solar cell in thermodynamic equilibrium. The diagram is shown for the p-n junction solar cell only (open system).

are matched by the opposite gradients and differences in the electric potential, so that the net potential across the p-n junction remains constant. This indicates that there is no preferential motion of the charge carriers, and, thus, no electric current.

Note that the same potential diagram plotted in Fig. 4 represents the situation for electrons as well as for holes, since the trends in the spatial distribution of the *potential* are identical for both types of particles (i.e. higher potential on the p-type side and lower on the n-type side). If we would plot the spatial distribution of the potential *energies*, however, two separate diagrams for electrons and holes would be required, one being an inverted image of the other, since for electrons the potential energy is higher on the n-type side, while for the holes it is higher on the p-type side. This is another reason why plotting potential diagrams is more convenient compared to energy diagrams, besides the fact that the fields and voltages can be discerned directly from potential gradients and potential differences, as already demonstrated.

When the p-n junction is connected to the outside world via metal contacts, similar chemical and electric forces arising from the differences in the concentration of the charge carriers appear also at the interfaces between the semiconductor and the metal, indicated by the subscript "m", so that $V^0_{\mathrm{net,nm}} = \mathcal{V}^0_{\mathrm{nm}} - V^0_{\mathrm{nm}} = 0$ at the n-type/metal contact, and $V^0_{\mathrm{net,pm}} = \mathcal{V}^0_{\mathrm{pm}} - V^0_{\mathrm{pm}} = 0$ at the p-type/metal contact. Further on, if we assume that a metal with the same work function is used on both sides of the p-n junction, the chemical voltages compensate each other exactly, so that $\mathcal{V}^0_{\mathrm{nm}} + \mathcal{V}^0_{\mathrm{pn}} + \mathcal{V}^0_{\mathrm{pm}} = 0$ and, consequently, also $V^0_{\mathrm{nm}} + V^0_{\mathrm{pn}} + V^0_{\mathrm{pm}} = 0$. There is zero resultant voltage between the terminals, and there is no current flowing through the circuit. This is demonstrated also by Fig. 4 in which it is clear that the electric potential does not differ between the two terminals of the device (points A and B), which confirms that there is no resultant voltage maintained across the structure. The system is in *complete thermodynamic equilibrium*.

### B. p-n junction under illumination

Under constant illumination the energy carried by the incident photons can be harvested to excite the bound electrons from the valence band to the conduction band, generating additional free electron-hole pairs. These photo-generated charge carriers are short-lived, however, and eventually recombine back to their bound state. In steady-state conditions, when the generation and the recombination rates are in balance, there exists an excess of charge carriers $\Delta n$ and $\Delta p$, and thus the total concentration is increased to $n^{\mathrm{L}} = n^0 + \Delta n$ and $p^{\mathrm{L}} = p^0 + \Delta p$. The superscript "L" indicates the illumination conditions.

As a results of the increased charge-carrier concentrations, the chemical potentials for the electrons and holes in general change as well, as given in Eq. 8.

$$\begin{aligned}\psi^{\mathrm{L}}_{\mathrm{e}} &= \frac{\tilde{\mu}_{\mathrm{e}}}{-q} + \frac{kT}{-q}\ln\frac{n^0+\Delta n}{N_{\mathrm{C}}} = \psi^0_{\mathrm{e}} - \frac{kT}{q}\ln\left(1+\frac{\Delta n}{n^0}\right)\\ \psi^{\mathrm{L}}_{\mathrm{h}} &= \frac{\tilde{\mu}_{\mathrm{h}}}{q} + \frac{kT}{q}\ln\frac{p^0+\Delta p}{N_{\mathrm{V}}} = \psi^0_{\mathrm{h}} + \frac{kT}{q}\ln\left(1+\frac{\Delta p}{p^0}\right)\end{aligned} \tag{8}$$

Focusing on the neutral regions of both semiconductor layers (i.e. far away from the junction), the changes of the chemical potential can be written separately for the electrons and holes, and further separately for the p-type and n-type layers, as follows:

$$\begin{aligned}\Delta\psi_{\mathrm{p,e}} &= -\frac{kT}{q}\ln\left(1+\frac{\Delta n_{\mathrm{p}}}{n^0_{\mathrm{p}}}\right) \qquad \Delta\psi_{\mathrm{n,e}} = -\frac{kT}{q}\ln\left(1+\frac{\Delta n_{\mathrm{n}}}{n^0_{\mathrm{n}}}\right)\\ \Delta\psi_{\mathrm{p,h}} &= \frac{kT}{q}\ln\left(1+\frac{\Delta p_{\mathrm{p}}}{p^0_{\mathrm{p}}}\right) \qquad \Delta\psi_{\mathrm{n,h}} = \frac{kT}{q}\ln\left(1+\frac{\Delta p_{\mathrm{n}}}{p^0_{\mathrm{n}}}\right)\end{aligned} \tag{9}$$

Since $\Delta n_{\mathrm{p}}/n^0_{\mathrm{p}} \gg \Delta n_{\mathrm{n}}/n^0_{\mathrm{n}}$ and $\Delta p_{\mathrm{n}}/p^0_{\mathrm{n}} \gg \Delta p_{\mathrm{p}}/p^0_{\mathrm{p}}$, it is evident that $|\Delta\psi_{\mathrm{p,e}}| > |\Delta\psi_{\mathrm{n,e}}|$ and $|\Delta\psi_{\mathrm{n,h}}| > |\Delta\psi_{\mathrm{p,h}}|$. The absolute change of the chemical potential is much greater on that side of the p-n junction where the observed type of charge carriers represents the *minority*, i.e., electrons in the p-type or holes in the n-type layer. Therefore, as an important consequence of this asymmetry, the chemical voltages across the p-n junction change as well under illumination:

$$\begin{aligned}\Delta\mathcal{V}_{\mathrm{pn,e}} &= \Delta\psi_{\mathrm{p,e}} - \Delta\psi_{\mathrm{n,e}} = \frac{kT}{q}\ln\frac{1+\Delta n_{\mathrm{n}}/n^0_{\mathrm{n}}}{1+\Delta n_{\mathrm{p}}/n^0_{\mathrm{p}}}\\ \Delta\mathcal{V}_{\mathrm{pn,h}} &= \Delta\psi_{\mathrm{p,h}} - \Delta\psi_{\mathrm{n,h}} = \frac{kT}{q}\ln\frac{1+\Delta p_{\mathrm{p}}/p^0_{\mathrm{p}}}{1+\Delta p_{\mathrm{n}}/p^0_{\mathrm{n}}}\end{aligned} \tag{10}$$

These changes collapse the balance of the voltages across the p-n junction and, thus, break the thermodynamic equilibrium. Both changes are *negative*, which means that the chemical voltages are *reduced*. However, since the voltages in the thermodynamic equilibrium are inherently balanced out, it is more convenient to interpret $\Delta\mathcal{V}_{\mathrm{pn,e}}$ and $\Delta\mathcal{V}_{\mathrm{pn,h}}$ as additional, illumination-induced voltages that are superimposed to the situation in the thermodynamic equilibrium. The flow of charge carriers is triggered under their influence, but they clearly act in the *opposite* direction of the initial $\mathcal{V}^0_{\mathrm{pn,e}}$ and $\mathcal{V}^0_{\mathrm{pn,h}}$; they drive electrons from the p-type into the n-type layer and holes from the n-type into the p-type layer. From this, *selectivity* of charge-carrier separation driven by these illumination-induced voltages is also revealed.

At this point it should be mentioned that in semiconductor materials, the illumination-induced changes of the chemical potentials of the charge carriers can be related to the changes of their (*quasi*-)Fermi energies, $\Delta E_{\mathrm{F}} = E^{\mathrm{L}}_{\mathrm{F}} - E^0_{\mathrm{F}}$, so that $\Delta\psi = \Delta E_{\mathrm{F}}/(-q)$. Note that this is true "immediately after" illumination, i.e., before the photo-generated charge carriers had the chance to separate, so that the electric potentials remained unchanged from the situation in thermodynamic equilibrium. In a conventional energy diagram in which $E^0_{\mathrm{F}}$ for both electrons and holes is taken as the reference in thermodynamic equilibrium, the illumination-induced voltages $\Delta\mathcal{V}_{\mathrm{pn,e}}$ and $\Delta\mathcal{V}_{\mathrm{pn,h}}$ can thus be visualized from the differences of the quasi-Fermi energies across the p-n junction; $\Delta\mathcal{V}_{\mathrm{pn,e}} = \left(E^{\mathrm{L}}_{\mathrm{F,p,e}} - E^{\mathrm{L}}_{\mathrm{F,n,e}}\right)/(-q)$ and $\Delta\mathcal{V}_{\mathrm{pn,h}} = \left(E^{\mathrm{L}}_{\mathrm{F,p,h}} - E^{\mathrm{L}}_{\mathrm{F,n,h}}\right)/(-q)$. The result is again negative for both types of charge carriers which once more confirms the selective nature of charge carrier separation.

As the electrons and holes begin to diffuse across the p-n junction under the influence of $\Delta\mathcal{V}_{\mathrm{pn,e}}$ and $\Delta\mathcal{V}_{\mathrm{pn,h}}$, their electric potentials begin to change as well. This results in the changes of the electric fields and the electric voltages. In open-circuit conditions, a new balance is eventually established, so that $V^{\mathrm{L}}_{\mathrm{net,pn}} = \mathcal{V}^{\mathrm{L}}_{\mathrm{pn}} - V^{\mathrm{L}}_{\mathrm{pn}} = \left(\mathcal{V}^0_{\mathrm{pn}} + \Delta\mathcal{V}_{\mathrm{pn}}\right) - \left(V^0_{\mathrm{pn}} + \Delta V_{\mathrm{pn}}\right) = 0$, which leads to $\Delta\mathcal{V}_{\mathrm{pn}} - \Delta V_{\mathrm{pn}} = 0$. Therefore, to compensate for the change of the chemical voltage, an additional electric voltage is generated across the p-n junction.

This *open-circuit voltage* can be expressed separately for electrons and holes as given in Eq. 11:

$$V_{\mathrm{OC,e}} = -\Delta V_{\mathrm{pn,e}} = -\Delta \mathcal{V}_{\mathrm{pn,e}} = \frac{kT}{q} \ln \frac{1 + \Delta n_{\mathrm{p}}/n_{\mathrm{p}}^0}{1 + \Delta n_{\mathrm{n}}/n_n^0}$$
$$V_{\mathrm{OC,h}} = -\Delta V_{\mathrm{pn,h}} = -\Delta \mathcal{V}_{\mathrm{pn,h}} = \frac{kT}{q} \ln \frac{1 + \Delta p_{\mathrm{n}}/p_n^0}{1 + \Delta p_{\mathrm{p}}/p_{\mathrm{p}}^0} \tag{11}$$

The complete potential diagram for the illuminated p-n junction solar cell in open-circuit conditions is presented in Fig. 5 (dashed blue lines), superimposed to the situation in thermodynamic equilibrium (full black lines). The changes of the chemical and electric potentials are in balance, while the net potential is constant throughout the structure. More importantly, it is clear that the electric voltage between the terminals of the solar cell equals the *change* of the electric potential across the p-n junction, which was induced by the change of the non-electric chemical voltage $\Delta\mathcal{V}_{\mathrm{pn}}$. The terminal at point B is at a higher electric potential than the one at point A (positive terminal on the p-side, negative on the n-side) – this voltage is oriented in the *opposite* direction to the "built-in" voltage $V_{\mathrm{pn}}^0$, which is crucial for a physically consistent interpretation of the generator nature of the illuminated p-n junction, as will be discussed later in relation to the Poynting vector.

The situation presented in Fig. 5 is completely analogous to that presented in Fig. 2, with the p-n junction solar cell now taking the place of the generalized electric source. The main difference is that in the case of the electric source the non-electric voltage was *increased*

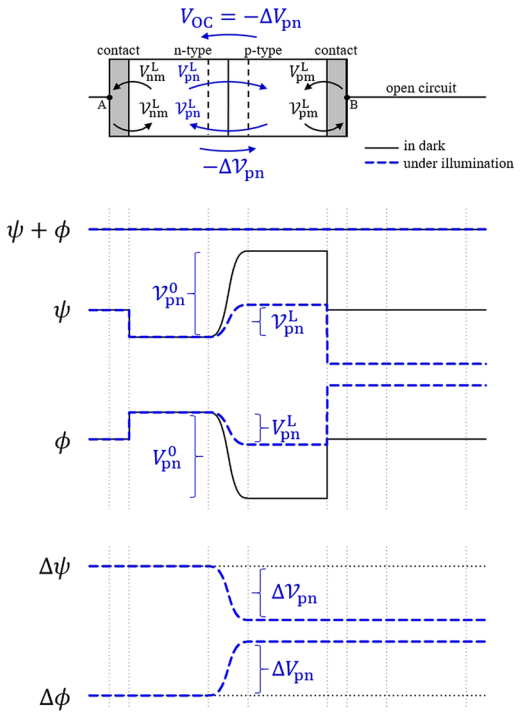


**FIG. 5**. Complete potential diagram of the p-n junction solar cell in thermodynamic equilibrium (full black lines), and under open-circuit conditions (dashed blue lines). The diagram is shown for the p-n junction solar cell only (open system).

once the generator action was enabled (from 0 to $\mathcal{V}^{\mathrm{G}}$; $\Delta\mathcal{V} > 0$), whereas in the case of the p-n junction solar cell the non-electric chemical voltage was *decreased* under illumination (from $\mathcal{V}_{\mathrm{pn}}^0$ to $\mathcal{V}_{\mathrm{pn}}^{\mathrm{L}}$; $\Delta\mathcal{V}_{\mathrm{pn}} < 0$). However, the *change* was, in both cases, oriented in the same direction – the chemical potential of the positive terminal B decreased with respect to the negative terminal A. This change of the non-electric voltage triggered the motion of the charge carriers and, thus, induced the open-circuit voltage in both devices.

Finally, note that the voltages $V_{\mathrm{OC,e}}$ and $V_{\mathrm{OC,h}}$ derived above and illustrated in Fig. 5 can each affect only one type of the photo-generated charge carriers, either electrons ($\Delta n_{\mathrm{p}}$ and $\Delta n_{\mathrm{n}}$) or holes ($\Delta p_{\mathrm{p}}$ and $\Delta p_{\mathrm{n}}$), respectively. This is the result of the independent theoretical treatment of the electrons and holes, as if they were traveling under separate "channels" inside the solar cell. In contrast, the realistic open-circuit voltage $V_{\mathrm{OC}}$ that can be experimentally measured between the terminals of the solar cell is induced under the influence of the entire pool of the photo-generated charge carriers. Therefore, its value can be calculated from the relative contributions of the charge carriers, as given in Eq. 12.

$$V_{\mathrm{OC}} = \frac{(\Delta n_{\mathrm{p}} + \Delta n_{\mathrm{n}})V_{\mathrm{OC,e}} + (\Delta p_{\mathrm{p}} + \Delta p_{\mathrm{n}})V_{\mathrm{OC,h}}}{\Delta n_{\mathrm{p}} + \Delta n_{\mathrm{n}} + \Delta p_{\mathrm{p}} + \Delta p_{\mathrm{n}}} \tag{12}$$

The equation can be further simplified by assuming that $\Delta n_{\mathrm{p}} = \Delta p_{\mathrm{p}}$ and $\Delta n_{\mathrm{n}} = \Delta p_{\mathrm{n}}$:

$$V_{\mathrm{OC}} = \frac{V_{\mathrm{OC,e}} + V_{\mathrm{OC,h}}}{2} = \frac{kT}{2q} \ln \frac{\left(1 + \Delta n_{\mathrm{p}}/n_{\mathrm{p}}^0\right)\left(1 + \Delta p_{\mathrm{n}}/p_{\mathrm{n}}^0\right)}{\left(1 + \Delta n_{\mathrm{n}}/n_{\mathrm{n}}^0\right)\left(1 + \Delta p_{\mathrm{p}}/p_{\mathrm{p}}^0\right)} \tag{13}$$

From this point onward we can draw an analogy with the generalized electric source discussed previously. When the illuminated p-n junction solar cell is loaded, the separated charge carriers can flow over the load, which results in a reduction of the voltage at the terminals, $V^{\mathrm{L}} = V_{\mathrm{OC}} - \delta V$. A new balance is established in which the current flowing over the load, driven by $V_{\mathrm{R}}$ and governed by the current-voltage characteristics of the load, matches the current over the illuminated p-n junction, driven by $\delta V$ and governed by its own current-voltage characteristics.

If the solar cell is put into the short-circuit conditions, $R \to 0$ and $V_{\mathrm{R}} \to 0$, the voltage over the p-n junction *inside* the solar cell would become $\delta V_{\mathrm{SC}} = V_{\mathrm{OC}}$, and it would drive the short-circuit current $I_{\mathrm{SC}}$ through the device. The open-circuit voltage $V_{\mathrm{OC}}$ of the illuminated p-n junction solar cell is thus related to the short-circuit current $I_{\mathrm{SC}}$ via the current-voltage characteristics of the p-n junction, in this case the well-known diode equation.

Fig. 6 shows the complete potential diagram plotted for the case of a loaded p-n junction (full red lines) and for the short-circuit conditions (dash-dotted green lines), superimposed to the plot from Fig. 5 for the open-circuit conditions (dashed blue lines). Note that the situation is again completely analogous to that presented in Fig. 3 for the case of the generalized electric source. The net potential is no longer constant; its gradients indicate the flow of the electric current. The current over the p-n junction is governed by $\delta V$, and that through the load by $V_{\mathrm{R}}$. In addition, from $\Delta\phi$ it is clear that the voltage between the terminals inside the solar cell is oriented in the opposite direction to the flowing current, which means that the Poynting vector is oriented outwards – the solar cell truly acts as a generator. And finally, in relation to the discussion in Section III, note that the net potential difference between the terminals of the

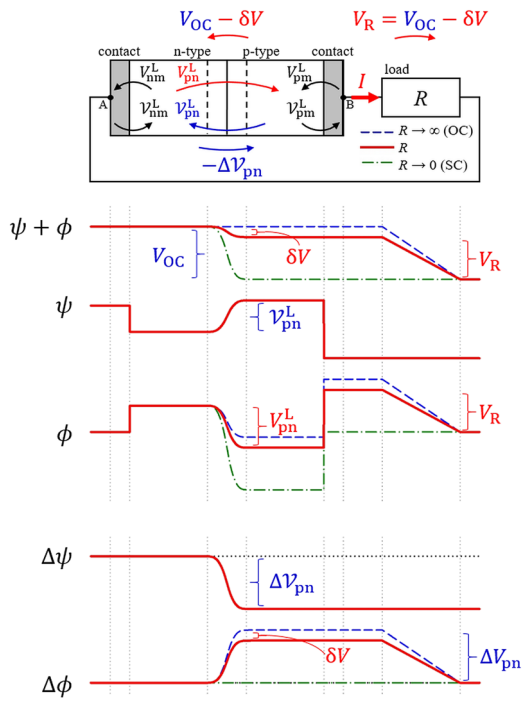


**FIG. 6**. Complete potential diagram of the p-n junction in thermodynamic equilibrium (full black lines), and under open-circuit conditions (dashed blue lines).

solar cell *does not* match the net potential difference across the load, since the net potential is non-conservative in nature.

In retrospect, we would like to emphasize once more that the generator properties of the solar cell discussed above are induced by the *change that the system experienced when stepping out from the thermodynamic equilibrium*. In the thermodynamic equilibrium, before illumination, all the forces, fields and voltages (including the "built-in" voltage $V^0_{pn}$) are in complete balance. Therefore, their magnitudes, polarities, and indeed even the existence itself are inconsequential with respect to the situation under illumination; they cannot be the drivers of an electric current, as they are inherently balanced out. Only a *change* from the thermodynamic equilibrium – in our case the change of the chemical voltage $\Delta\mathcal{V}_{pn}$ – can break the balance and induce the charge carriers to flow. In this *change*, therefore, we recognize the driving force that is able to selectively separate the charge carriers, induce the voltage at the terminals and, if the solar cell is connected to a load, maintain a constant current flowing out of the device and through the load.

## V. CONCLUSIONS

We presented a physically consistent interpretation of charge-carrier separation in p-n junction solar cells, following an analogy with a generalized electric source model. We introduced the complete potential diagram in which the spatial distributions of both the chemical potential and the electric potential are plotted. From their gradients and differences, the motion of charge carriers and the voltages inside the structure can be visualized, respectively. We showed that under illumination the balance between the non-electric diffusion forces and the electric forces is broken due to the non-equal change of the chemical potential of the free carriers on each side of the p-n junction, resulting in a decrease of the chemical voltage. This *change* of the non-electric chemical voltage is recognized as the driving force that triggers the selective charge-carrier separation across the p-n junction and, thus, induces the open-circuit voltage to appear at the terminals of the illuminated solar cell.

## ACKNOWLEDGMENTS

The authors acknowledge the financial support from the Slovenian Research Agency (research core funding No. P2-0197 and P2-0246).

## REFERENCES

[1] "Photovoltaics Report," Fraunhofer Institute for Solar Energy Systems ISE. Available: https://www.ise.fraunhofer.de/en/publications/studies/photovoltaics-report.html. (accessed: 4th February 2019).
[2] A. Cuevas and D. Yan, "Misconceptions and misnomers in solar cells," IEEE J. Photovoltaics **3**, 916 (2013).
[3] U. Würfel, A. Cuevas, and P. Würfel, "Charge carrier separation in solar cells," IEEE J. Photovoltaics **5**, 461 (2015).
[4] P. Würfel and U. Würfel, *Physics of Solar Cells: From Basic Principles to Advanced Concepts*, 3rd Ed (Wiley-VCH, 2016).
[5] M. A. Green, "Photovoltaic principles," Physica E **14**, 11 (2002).
[6] K. O. Hara and N. Usami, "Theory of open-circuit voltage and the driving force of charge separation in pn-junction solar cells," J. Appl. Phys. **114**, 153101 (2013).
[7] T. Kirchartz, J. Bisquert, I. Mora-Sero, and G. Garcia-Belmonte, "Classification of solar cells according to mechanisms of charge separation and charge collection," Phys. Chem. Chem. Phys. **17**, 4007 (2015).
[8] G. H. Bauer, *Photovoltaic Solar Energy Conversion* (Springer Berlin Heidelberg, 2015).
[9] G. Job and F. Herrmann, "Chemical potential—A quantity in search of recognition," Eur. J. Phys. **27**, 353 (2006).
[10] C. H. Page, "Electromotive force, potential difference, and voltage," Am. J. Phys. **45**, 978 (1977).
[11] R. H. Romer, "What do 'voltmeters' measure?: Faraday's law in a multiply connected region," Am. J. Phys. **50**, 1089 (1982).
[12] I. Riess, "What does a voltmeter measure?," Solid State Ionics **95**, 327 (1997).